INCLUSIVE DIFFRACTION AND LEADING BARYON PRODUCTION AT HERA

THOMAS NUNNEMANN
FOR THE H1 AND ZEUS COLLABORATIONS
Max-Plank-Institut für Kernphysik, Saupfercheckweg 1, 69117 Heidelberg, Germany
E-mail: Thomas.Nunnemann@mpi-hd.mpg.de

Recent H1 and ZEUS data on diffractive deep inelastic scattering and leading baryon production are reviewed.

1 Introduction

Large rapidity gap events and events with a high energetic proton or neutron have been observed at the ep–collider HERA.[1,3,2,4] The dynamical mechanisms for these reactions are only poorly understood within QCD. Whilst standard fragmentation models[5,6] are successful in describing energy flow in the photon fragmentation region, they fail to reproduce rates and energy distributions of leading baryons. In particular these models do not produce the excess of very energetic protons (close to the kinematical limit) or equivalently single diffractive dissociative events, which are characterized by a large rapidity gap.

Diffractive dissociation at high energies has been successfully described by the exchange of the leading vacuum singularity called the *pomeron* $I\!P$. In addition to virtual photon–pomeron interactions one also expects meson exchanges to contribute to the total deep inelastic scattering (DIS) cross section and to the production of leading baryons. Assuming a simple Regge expansion, the contribution of a colour singlet exchange with trajectory $\alpha(t)$ to the production of a leading baryon with fractional energy z is of the form $\sim (1-z)^{1-2\alpha(t)}$. Thus $I\!P$ exchange ($\alpha_{I\!P}(0) \sim 1.1$) is expected to dominate the production cross section for protons with energies close to the proton beam energy, whereas reggeon ($\alpha_{I\!R}(0) \sim 0.5$) and pion exchange ($\alpha_\pi(0) \sim 0$) are of increasing importance at lower values of z. Neutron production can only occur through the exchange of an an isovector particle, notably the π^+. In DIS at HERA one has the excellent opportunity to study the short distance structure of the exchanged objects.[7,8,9]

An alternative approach to describe the production of leading baryons without Regge dynamics is the soft colour interaction model which is implemented in the LEPTO Monte Carlo program.[10] In this model the colour topology of the final state is modified by an exchange of soft gluons leading to a colour separation between the current and target fragmentation regions.

2 Kinematics

The process of diffractive DIS is sketched in Figure 1. Denoting the four–vectors of the incoming photon and proton with q and p respectively, two independent inclusive kinematic variables can be defined as

$$Q^2 = -q^2 \ , \qquad\qquad W^2 = (q+p)^2 \ . \tag{1}$$

It is convenient also to define the dimensionless scaling variables

$$x = \frac{Q^2}{2p \cdot q} , \qquad y = \frac{p \cdot q}{p \cdot k} , \tag{2}$$

where k is the four–vector of the incoming electron. The hadronic final state of any event may be decomposed into two systems X and Y (with invariant masses M_X and M_Y) which are separated by the largest gap in the rapidity[a] distribution of the hadronic final state. In case of single dissociation or leading baryon production the system Y is a single proton or neutron.

Kinematic variables describing the hadronic final state are defined as

$$x_{\mathbb{P}} = \frac{q \cdot (p - p_Y)}{q \cdot p} , \qquad t = (p - p_Y)^2 , \tag{3}$$

where p_Y denotes the four–momentum of the system Y. In the colour–singlet–exchange picture $x_{\mathbb{P}}$ can be interpreted as the fraction of the proton beam momentum transferred to the exchanged object, with t being its four–momentum squared. $\beta = x/x_{\mathbb{P}}$ is then the corresponding Bjorken–variable for scattering off the exchanged object.

Where leading baryons are detected, the energy E' and transverse momentum p_T of the final state proton or neutron is used to define the semi–inclusive variables

$$z = 1 - \frac{q \cdot (p - p_Y)}{q \cdot p} \simeq \frac{E'}{E} , \tag{4}$$

$$\begin{aligned} t &= (p - p')^2 \\ &\simeq \frac{p_T^2}{z} - (1 - z)\left(\frac{m_N^2}{z} - m_p^2\right) , \end{aligned} \tag{5}$$

where p' is the four–vector of the final–state nucleon and m_N is its mass. Provided the final–state nucleon is exclusively produced at the proton vertex, the definitions (3) and (5) of t are equivalent and $z = 1 - x_{\mathbb{P}}$.

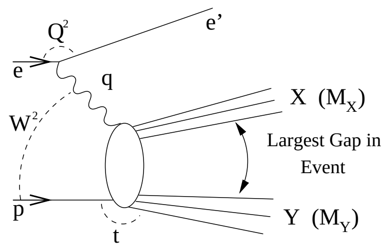

Figure 1. Sketch of the diffractive ep interaction.

3 Experimental Techniques

Different methods to select diffractive dissociation are employed by the two collaborations:

- Large Rapidity gap selection: Since no colour field is connecting the two hadronic subsystems X and Y, diffractive events are characterized by a rapidity gap of the size $\Delta\eta \simeq \ln \frac{W^2}{M_X^2}$. In the H1 selection the gap is identified by an absence of activity in the forward[b] part of the detector ($3.3 \leq \eta \leq 7.5$).[11] The required size of the rapidity gap restricts the measurement to the region $x_{\mathbb{P}} \lesssim 0.05$ in which diffraction is expected to be dominant. Since the system

[a] Rapidity is approximated by pseudo–rapidity which is defined as $\eta = -\ln\tan\frac{\theta}{2}$.
[b] At HERA the forward direction is that of the outgoing proton beam.

Y is not detected the resulting data sample effectively contains events with $M_Y < 1.6\,\mathrm{GeV}$.

- M_X subtraction method: The ZEUS collaboration extracts the diffractive signal from the distribution in the hadronic mass M_X without explicitly requiring a forward rapidity gap.[12] The hadronic mass distribution is fitted to the form

$$\frac{\mathrm{d}N}{\mathrm{d}\ln M_X^2} = D + c\,e^{b\ln M_X^2}\ , \tag{6}$$

  where D represents the diffractive contribution and the second term parameterizes the non–diffractive contribution which is exponentially suppressed at low M_X. Due to the smaller forward acceptance of their detector, the ZEUS measurement of the diffractive cross section is integrated over the range $M_Y < 5.5\,\mathrm{GeV}$.

- Detection of the leading baryon: Both experiments have dedicated forward proton spectrometers (FPS or LPS) and neutron calorimeters (FNC) to directly detect and measure protons and neutrons which are produced at very small scattering angles ($\theta \lesssim 1\,\mathrm{mrad}$).[2,3,4] This method enhances the kinematic range in $x_{I\!P}$ to much larger values (see Section 5).

4 Diffractive Dissociation in DIS

4.1 Inclusive Cross Section Measurements

The dependence of the photon dissociation cross section on t has been measured in the region $x_{I\!P} < 0.03$.[13] It is found to be described by an exponential shape $\mathrm{d}\sigma/\mathrm{d}t \propto e^{bt}$ with the slope parameter $b = 7.1 \pm 1.0\,(\mathrm{stat.}) \pm 1.2\,(\mathrm{syst.})\,\mathrm{GeV}^{-2}$, which is demonstrated in Figure 2. This large value is characteristic for a highly peripheral scattering process.

In analogy to inclusive DIS, the photon dissociative cross section, integrated over the measured range in t and M_Y, can be parameterized with a three–fold diffractive structure function $F_2^{D(3)}(\beta, Q^2, x_{I\!P})$:

$$\frac{\mathrm{d}^3\sigma}{\mathrm{d}\beta\,\mathrm{d}Q^2\,\mathrm{d}x_{I\!P}} = \frac{4\pi\alpha^2}{\beta Q^4}\left(1 - y + \frac{y^2}{2}\right) F_2^{D(3)}(\beta, Q^2, x_{I\!P})\ . \tag{7}$$

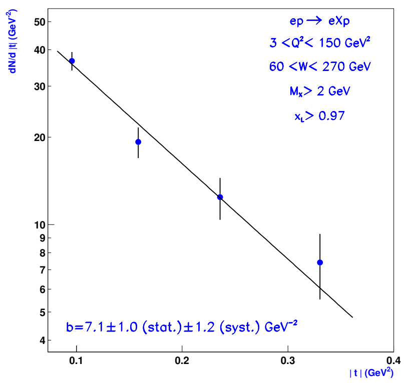

Figure 2. Differential t–distribution obtained with the ZEUS LPS.

When comparing measurements of $F_2^{D(3)}$ which are based on different selection methods as described in the previous section, one should be cautious that they cover different ranges in M_Y. Figure 3 shows a comparison of results obtained by ZEUS with the M_X–subtraction method[12] ($M_Y < 5.5\,\mathrm{GeV}$) and by using the Leading Proton Spectrometer LPS[2] ($M_Y = M_p$) and the H1 measurement based on the rapidity gap selection[11] ($M_Y < 1.6\,\mathrm{GeV}$). The H1 and ZEUS (LPS) measurements are in good agreement, whereas the ZEUS (M_X) result is significantly larger for $Q^2 \leq 9\,\mathrm{GeV}^2$. By comparing their two analysis the ZEUS Collaboration estimates a contribution of double dissociation for the M_X–measurement of $(31 \pm 15)\%$.[12]

Assuming the diffractive cross section is due to pomeron exchange only, a factorization of the $x_{\mathrm{I\!P}}$ dependence of $F_2^{D(3)}$ is expected of the form[7]

$$F_2^{D(3)}(\beta, Q^2, x_{\mathrm{I\!P}}) = f_{\mathrm{I\!P}/p}(x_{\mathrm{I\!P}}) F_2^{\mathrm{I\!P}}(\beta, Q^2) \qquad (8)$$

where the pomeron flux factor integrated over t is given by

$$f_{\mathrm{I\!P}/p}(x_{\mathrm{I\!P}}) = \int_{t_{max}}^{t_{min}(x_{\mathrm{I\!P}})} \mathrm{d}t\, x_{\mathrm{I\!P}}^{1-2\alpha_{\mathrm{I\!P}}(t)} e^{b_0 t}\,. \quad (9)$$

In equation 8, $F_2^{\mathrm{I\!P}}(\beta, Q^2)$ may be interpreted as being proportional to the structure function of the pomeron.

The ZEUS(M_X)–measurement, which is restricted to $x_{\mathrm{I\!P}} < 0.01$ is consistent with this factorization and a universal $x_{\mathrm{I\!P}}$–dependence corresponding to a t–averaged pomeron trajectory of $\overline{\alpha_{\mathrm{I\!P}}} = 1.127 \pm 0.009\,(\mathrm{stat.})^{+0.039}_{-0.012}\,(\mathrm{syst.})$.[12]

The H1 measurement, which extend to larger values of $x_{\mathrm{I\!P}}$ ($x_{\mathrm{I\!P}} < 0.04$), break the factorization given in equation 8. When also considering the exchange of a further trajectory, the *reggeon* $\mathrm{I\!R}$, in addition to the pomeron one gets a good description of $F_2^{D(3)}$ throughout the measured range, spanning the region $0.001 < \beta < 0.9$ and $0.4\,\mathrm{GeV}^2 < Q^2 < 800\,\mathrm{GeV}^2$.[11,16] The $\mathrm{I\!R}$ contribution is of particular importance in the region of large $x_{\mathrm{I\!P}}$ and low β. Fits to the intermediate Q^2–data yield $\alpha_{\mathrm{I\!P}}(0) = 1.203 \pm 0.020\,(\mathrm{stat.}) \pm 0.013\,(\mathrm{syst.})^{+0.030}_{-0.035}\,(\mathrm{model})$ and for the intercept of the secondary trajectory $\alpha_{\mathrm{I\!R}}(0) = 0.50 \pm 0.11\,(\mathrm{stat.}) \pm 0.11\,(\mathrm{syst.})^{+0.09}_{-0.10}\,(\mathrm{model})$ consistent with the exchange of the f_2 and its degenerate partners.[11]

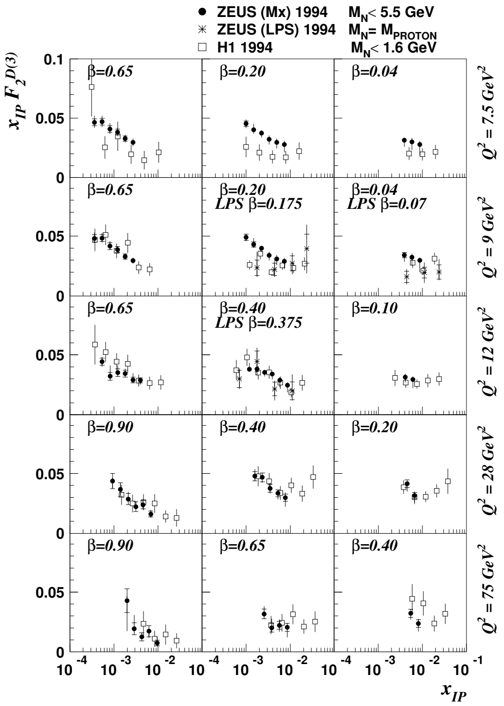

Figure 3. $x_{\mathrm{I\!P}} F_2^{D(3)}(\beta, Q^2, x_{\mathrm{I\!P}})$ as a function of $x_{\mathrm{I\!P}}$ for different values of β and Q^2. Shown is a comparison of the measurements obtained by ZEUS and H1, which cover different ranges in M_Y (here denoted as M_N).

The ZEUS measurement of the effective pomeron trajectory extrapolated to $\alpha_{\mathrm{I\!P}}(0) \simeq \overline{\alpha_{\mathrm{I\!P}}} + 0.03$ is consistent with the intercept determined by H1 and both results are significantly larger than the value $\alpha_{\mathrm{I\!P}}(0) \approx 1.08$ obtained from soft hadron–hadron interactions.[15]

4.2 Partonic Structure of Diffraction

In contrast to the proton structure, scaling violations in the diffractive structure function with positive $\mathrm{d}F_2^{D(3)}/\mathrm{d}\ln Q^2$ persists to large values of $\beta = 0.4$ indicating a large gluon component in the structure of the diffractive exchange. A QCD analysis of $F_2^{D(3)}$ using NLO DGLAP[17] evolution equations confirms this qualitative picture. The resulting fraction of the momentum of the pomeron carried by gluons amounts to $\sim 90\%$ at $Q^2 = 4.5\,\mathrm{GeV}^2$ decreasing to $\sim 80\%$ at $Q^2 = 75\,\mathrm{GeV}^2$.[11]

Various analysis of the hadronic final state in diffractive DIS (hadronic energy flow, multiplicity structure, dijet production) support the prediction of a gluonic pomeron providing a global consistent picture of diffraction.[18]

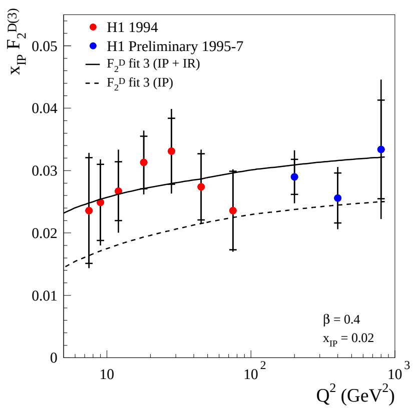

Figure 4. Q^2 dependence of $x_{\mathbb{P}}F_2^{D(3)}$ at $\beta = 0.4$ and $x_{\mathbb{P}} = 0.02$. The results of a QCD fit to the 1994 data in which both quarks and gluons contribute at the starting scale for evolution are also shown.

5 Leading Proton and Neutron Production

The production of leading nucleons has been studied over a wide kinematic range in z by H1 and ZEUS. As an example the ZEUS measurement of the z–distribution for both protons and neutrons is shown in figure 5.[14] Integrated over fractional energies $0.6 < z < 0.9$ and scattering angles $\theta < 0.8\,\mathrm{mrad}$ they find a production rate for leading nucleons of $\sim 12.5\%$. As demonstrated in the figure standard fragmentation models like the colour dipole model, which is implemented in the ARIADNE MC,[5] cannot describe the rate and energy–shape of leading baryons.

H1 has measured the semi–inclusive cross sections for DIS events with a high–energy proton with $0.7 \le z \le 0.9$ and for events with an energetic neutron with $0.2 \le z \le 1$ in the kinematic region $2 \le Q^2 \le 50$ GeV^2, $0.00006 \le x \le 0.0060$ and $p_T \le 0.2\,\mathrm{GeV}$.[4] The cross sections are parameterized in terms of semi–inclusive structure functions $F_2^{LB(3)}$ (where LB stands for either leading proton (LP) or neutron (LN)), which are defined in close analogy to the inclusive and diffractive structure functions:

$$\frac{\mathrm{d}^3\sigma(ep \to e'NX)}{\mathrm{d}x\,\mathrm{d}Q^2\,\mathrm{d}z} = \frac{4\pi\alpha^2}{x\,Q^4}(1 - y + \frac{y^2}{2})F_2^{LB(3)}(x, Q^2, z)\ . \tag{10}$$

The results for $F_2^{LN(3)}$ are shown in figure 5. In all bins the data fall with increasing z and a rise of $F_2^{LN(3)}$ with increasing Q^2 has been observed. The pion–exchange model simulated by RAPGAP agrees with the data only for $z \ge 0.7$. Despite its good description of the neutron data, LEPTO underestimates the rate of leading proton production and its rise with Q^2.

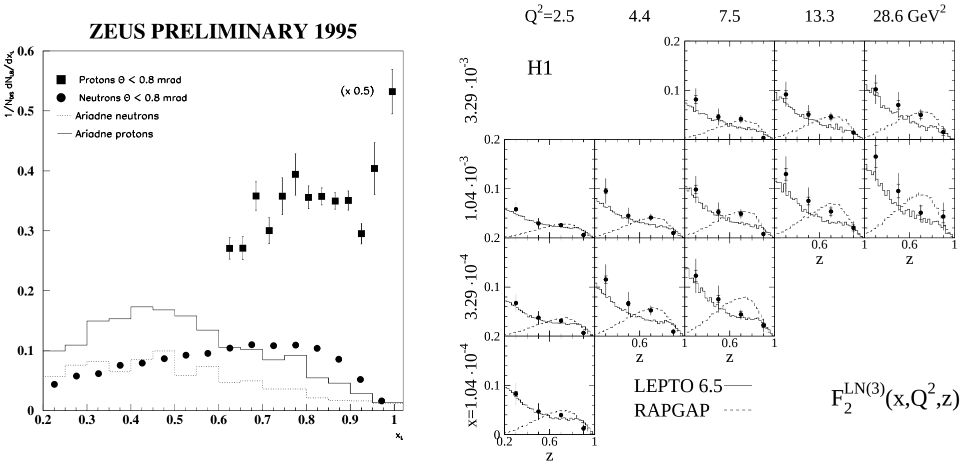

Figure 5. Left: z–spectrum ($x_L = z$) for protons and neutrons with scattering angles $\theta < 0.8$ mrad compared to the predictions of ARIADNE. Right: The semi–inclusive structure function $F_2^{LN(3)}$ for neutrons with $p_T < 0.2$ GeV compared to the predictions of LEPTO and RAPGAP.

5.1 A Regge Model of Baryon Production

In the region $z \geq 0.7$, H1 compares their measurements of the leading baryon structure functions $F_2^{LB(3)}$ to a Regge model which is based on $\mathbb{P}$, $\mathbb{R}$ and π exchange. The contribution of each colour singlet $\mathcal{P}$ is determined by the particle flux $f_{\mathcal{P}/p}(z, p_T)$ and its structure function $F_2^{\mathcal{P}}(\beta, Q^2)$:

$$F_2^{LB(3)}(\beta, Q^2, z) = \sum_{\mathcal{P}} \left\{ \int_{p_T=0\,\mathrm{GeV}}^{p_T=0.2\,\mathrm{GeV}} \mathrm{d}p_T\, f_{\mathcal{P}/p}(z, p_T) \right\} \cdot F_2^{\mathcal{P}}(\beta, Q^2)\ . \qquad (11)$$

The exchange of isovector reggeons (a_2, ω), which can contribute to neutron production, is neglected, since there is no evidence for them in the data, and because they have been estimated to be much smaller than the contribution of the isoscalar reggeons.[20] The flux factors have been determined using hadron–hadron data.[21,20] For F_2^{π} the GRV-LO parameterization[22] is used, and following reference[21] it is assumed that $F_2^{\mathbb{R}} = F_2^{\pi}$ and $F_2^{\mathbb{P}} = 0.22 F_2^{\mathbb{R}}$ at low β.

The breakdown of the cross section into different exchange contributions is shown in figure 6. Leading neutron production with $z \geq 0.7$ can be described by π^+ exchange alone whereas for the proton data, reggeon exchange contributes approximately 2/3 of the cross–section.

This Regge model is also consistent with the z–dependence of the slope parameter b, obtained by fitting the ZEUS leading proton data to the exponential form $\mathrm{d}\sigma/\mathrm{d}t \propto e^{bt}$ (see figure 6).[14]

5.2 The Pion Structure Function

Since within the Regge model the leading neutron cross section is saturated by π–exchange only, the measurement of $F_2^{LN(3)}$ at $z = 0.7$ and the p_T integrated pion

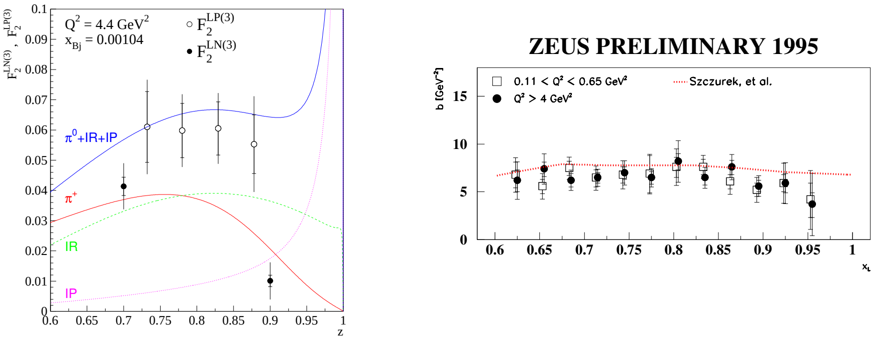

Figure 6. Left: z–dependence of the leading proton and neutron structure functions in an example bin of x and Q^2. The data is compared to a Regge model, of which the decomposition into the different contributions is superimposed. The contribution of π^0 exchange, which is not shown, is exactly half of the π^+ contribution. Right: Dependence of the t–slope parameter on z compared to a similar model.

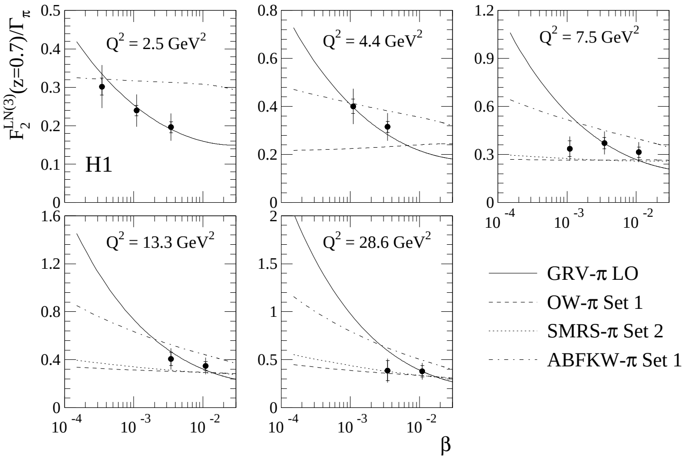

Figure 7. $F_2^{LN(3)}/\Gamma_\pi$ at $z = 0.7$ plotted as a function of β for fixed values of Q^2. The data, which may be interpreted as being equal to the pion structure function F_2^π are compared to different parameterizations of F_2^π.

flux factor $\Gamma_\pi(z) = \int \mathrm{d}p_T\, f_{\pi/p}(z, p_T)$ can be used to estimate the pion structure function F_2^π at low values of β:

$$F_2^\pi(\beta, Q^2) \approx F_2^{LN(3)}(\beta, Q^2, z = 0.7)/\Gamma_\pi(z = 0.7) \ . \qquad (12)$$

The estimate of F_2^π within this model is shown in figure 7 in a previously unexplored low β region. The GRV-LO parameterization[22] is consistent with the data.

6 Conclusions

Over the last years, the HERA experiments H1 and ZEUS have produced many results concerning diffraction and leading baryon production. These data can be successfully described with colour singlet exchange models, which offers the possibility to study the DIS structure of the exchanged objects.

References

1. ZEUS Collaboration, M. Derrick et al., *Phys. Lett.* **B315**, 481 (1993);
   H1 Collaboration, T. Ahmed et al., *Nucl. Phys.* **B429**, 477 (1994).
2. ZEUS Collaboration, J. Breitweg et al., *Eur. Phys. J.* **C1**, 81 (1998).
3. ZEUS Collaboration, M. Derrick et al., *Phys. Lett.* **B384**, 388 (1996).
4. H1 Collaboration, C. Adloff et al., *Eur. Phys. J.* **C6**, 587 (1999).
5. L. Lönnblad, *Comput. Phys. Comm.* **71**, 15 (1992).
6. T. Sjöstrand, *Comput. Phys. Comm.* **82**, 74 (1994).
7. G. Ingelman and P.E. Schlein, *Phys. Lett.* **B152**, 256 (1985).
8. H. Holtmann et al., *Phys. Lett.* **B338**, 363 (1994).
9. B. Kopeliovich, B. Povh and I. Potashnikova, *Z. Phys.* **C73**, 125 (()1996).
10. G. Ingelman, A. Edin and J. Rathsman, *Comp. Phys. Comm.* **101**, 108 (1997).
11. H1 Collaboration, C. Adloff et al., *Z. Phys.* **C76**, 613 (1997).
12. ZEUS Collaboration, J. Breitweg et al., *Eur. Phys. J.* **C6**, 43 (1999).
13. ZEUS Collaboration, Conf. Paper 972, 29th Intern. Conf. on HEP, Vancouver, Canada (1998).
14. ZEUS Collaboration, Conf. Paper 789, 29th Intern. Conf. on HEP, Vancouver, Canada (1998).
15. A. Donnachie and P.V. Landshoff, *Phys. Lett.* **B296**, 227 (1992)
16. H1 Collaboration, Conf. Paper 571, 29th Intern. Conf. on HEP, Vancouver, Canada (1998).
17. Yu. L. Dokshitser, *Sov. Phys. JETP* **46**, 641 (1977);
    V. N. Gribov and L. N. Lipatov, *Sov. J. Nucl. Phys.* **15**, 438 (1972);
    G. Altarelli and G. Parisi, *Nucl. Phys.* **B126**, 298 (1977).
18. H1 Collaboration, C. Adloff et al., *Phys. Lett.* **B428**, 206 (1998);
    H1 Collaboration, C. Adloff et al., *Eur. Phys. J.* **C5**, 439 (1998);
    ZEUS Collaboration, J. Breitweg et al., *Eur. Phys. J.* **C5**, 41 (1998);
    H1 Collaboration, C. Adloff et al., *Eur. Phys. J.* **C6**, 421 (1999).
19. H. Jung, *Comp. Phys. Comm.* **86**, 147 (1995).
20. K. Golec-Biernat, J. Kwiecinski, and A. Szczurek *Phys. Rev.* **D56**, 3955 (1997).
21. A. Szczurek, N.N. Nikolaev and J. Speth, *Phys. Lett.* **B428**, 383 (1998).
22. M. Glück, E. Reya and A. Vogt, *Z. Phys.* **C53**, 651 (1992).